

University of Groningen

Distributed control of power networks

Trip, Sebastian

IMPORTANT NOTE: You are advised to consult the publisher's version (publisher's PDF) if you wish to cite from it. Please check the document version below.

Document Version

Publisher's PDF, also known as Version of record

Publication date:

2017

[Link to publication in University of Groningen/UMCG research database](#)

Citation for published version (APA):

Trip, S. (2017). *Distributed control of power networks: Passivity, optimality and energy functions*. [Thesis fully internal (DIV), University of Groningen]. Rijksuniversiteit Groningen.

Copyright

Other than for strictly personal use, it is not permitted to download or to forward/distribute the text or part of it without the consent of the author(s) and/or copyright holder(s), unless the work is under an open content license (like Creative Commons).

The publication may also be distributed here under the terms of Article 25fa of the Dutch Copyright Act, indicated by the "Taverne" license. More information can be found on the University of Groningen website: <https://www.rug.nl/library/open-access/self-archiving-pure/taverne-amendment>.

Take-down policy

If you believe that this document breaches copyright please contact us providing details, and we will remove access to the work immediately and investigate your claim.

Downloaded from the University of Groningen/UMCG research database (Pure): <http://www.rug.nl/research/portal>. For technical reasons the number of authors shown on this cover page is limited to 10 maximum.

Published in:

S. Trip, M. Cucuzella, C. De Persis, A.J. van der Schaft and A. Ferrara – “Passivity based design of sliding modes for optimal Load Frequency Control,” 2017, under review.

M. Cucuzella, S. Trip, C. De Persis and A. Ferrara – “Distributed second order sliding modes for Optimal Load Frequency Control,” Proceedings of the 2017 American Control Conference (ACC), pp. 3451–3456, Seattle, WA, USA, 2017.

Chapter 6

Passivity based design of sliding modes

Abstract

This chapter proposes a distributed sliding mode control strategy for optimal Load Frequency Control (OLFC) in power networks, where besides frequency regulation also minimization of generation costs is achieved (economic dispatch). We study a nonlinear power network partitioned into control areas, where each area is modelled by an equivalent generator including voltage and second order turbine-governor dynamics. Desired passivity properties of the turbine-governor suggest the design of a sliding manifold, such that the turbine-governor system is passive once the sliding manifold is attained. This chapter offers a new perspective on OLFC by means of sliding mode control, and in comparison with the previous chapter, we relax required assumptions on the system parameters.

6.1 Control areas with second order turbine-governor dynamics

The considered model in this chapter extends the control area model studied in Chapter 2, with the second order turbine-governor dynamics discussed in Section 5.5. For convenience we will recall the associated dynamics and state the previously established incremental passivity property of the control area model in a slightly different manner. Consequently, we again consider a power network consisting of n interconnected control areas. The network topology is represented by a connected and undirected graph $\mathcal{G} = (\mathcal{V}, \mathcal{E})$, where the nodes $\mathcal{V} = \{1, \dots, n\}$, represent the control areas and the edges $\mathcal{E} = \{1, \dots, m\}$, represent the transmission lines connecting the areas. The topology can be described by its corresponding incidence matrix $B \in \mathbb{R}^{n \times m}$. Then, by arbitrarily labeling the ends of edge k with a $+$ and a $-$, one

has that

$$\mathcal{B}_{ik} = \begin{cases} +1 & \text{if } i \text{ is the positive end of } k \\ -1 & \text{if } i \text{ is the negative end of } k \\ 0 & \text{otherwise.} \end{cases}$$

A control area is represented by an equivalent generator and a load, where the governing dynamics of the i -th area are described by the so called ‘flux-decay’ or ‘single-axis model’ given as (Machowski et al. 2008):

$$\begin{aligned} \dot{\delta}_i &= \omega_i \\ T_{pi}\dot{\omega}_i &= -\omega_i + K_{pi} \left(\sum_{j \in \mathcal{N}_i} V_i V_j B_{ij} \sin(\delta_i - \delta_j) - P_{di} + P_{ti} \right) \\ T_{Vi}\dot{V}_i &= \bar{E}_{fi} - (1 - (X_{di} - X'_{di})B_{ii})V_i - (X_{di} - X'_{di}) \sum_{j \in \mathcal{N}_i} V_j B_{ij} \cos(\delta_i - \delta_j), \end{aligned} \quad (6.1)$$

where \mathcal{N}_i is the set of control areas connected to the i -th area by transmission lines. Moreover, P_{ti} in (6.1) is the power generated by the i -th (equivalent) plant and can be expressed as the output of the following second order dynamical system that describes the behaviour of both the governor and the turbine:

$$\begin{aligned} T_{ti}\dot{P}_{ti} &= -P_{ti} + P_{gi} \\ T_{gi}\dot{P}_{gi} &= -\frac{1}{K_i}\omega_i - P_{gi} + u_i. \end{aligned} \quad (6.2)$$

The symbols used in (6.1) and (6.2) are described in Table 6.1. We aim at the design of a continuous control input u_i to achieve both frequency regulation and economic efficiency (optimal Load Frequency Control).

To study the power network we write system (6.1) compactly for all areas $i \in \mathcal{V}$ as

$$\begin{aligned} \dot{\eta} &= \mathcal{B}^T \omega \\ T_p \dot{\omega} &= -\omega + K_p(P_t - P_d - \mathcal{B}\Gamma(V) \sin(\eta)) \\ T_V \dot{V} &= -(X_d - X'_d)E(\eta)V + \bar{E}_f, \end{aligned} \quad (6.3)$$

and the turbine-governor dynamics in (6.2) as

$$\begin{aligned} T_t \dot{P}_t &= -P_t + P_g \\ T_g \dot{P}_g &= -K^{-1}\omega - P_g + u, \end{aligned} \quad (6.4)$$

where $\eta = \mathcal{B}^T \delta \in \mathbb{R}^m$ is vector describing the differences in voltage angles. Furthermore, $\Gamma = \text{diag}\{\Gamma_1, \dots, \Gamma_m\}$, where $\Gamma(V)_k = V_i V_j B_{ij}$, with $k \sim \{i, j\}$, i.e., line k

State variables	
δ_i	Voltage angle
ω_i	Frequency deviation
V_i	Voltage
P_{ti}	Turbine output power
P_{gi}	Governor output
Parameters	
T_{pi}	Time constant of the control area
T_{ti}	Time constant of the turbine
T_{gi}	Time constant of the governor
T_{Vi}	Direct axis transient open-circuit constant
K_{pi}	Gain of the control area
K_i	Speed regulation coefficient
X_{di}	Direct synchronous reactance
X'_{di}	Direct synchronous transient reactance
B_{ij}	Transmission line susceptance
Inputs	
u_i	Control input to the governor
\bar{E}_{fi}	Constant exciter voltage
P_{di}	Unknown power demand

Table 6.1: Description of the used symbols

connects areas i and j . The components of the matrix $E(\eta) \in \mathbb{R}^{m \times m}$ are defined as

$$\begin{aligned}
 E_{ii}(\eta) &= \frac{1}{X_{di} - X'_{di}} - B_{ii} & i \in \mathcal{V} \\
 E_{ij}(\eta) &= B_{ij} \cos(\eta_k) = E_{ji}(\eta) & k \sim \{i, j\} \in \mathcal{E} \\
 E_{ij}(\eta) &= 0 & \text{otherwise.}
 \end{aligned} \tag{6.5}$$

The remaining symbols follow straightforwardly from (6.1) and (6.2), and are vectors and matrices of suitable dimensions. To permit the controller design in the next sections, the following assumption is made on the *unknown* demand (unmatched disturbance) and the available measurements:

Assumption 6.1.1 (Available information). *The variables ω_i , P_{ti} and P_{gi} are locally available at control area i . The unmatched disturbance P_{di} is unknown, and can be bounded as*

$$|P_{di}| \leq \mathcal{D}_i, \tag{6.6}$$

where \mathcal{D}_i is a positive constant available at control area i .

Before recalling the incremental passivity property for the considered power network model, we first need the following assumption on the existence of a steady state solution.

Assumption 6.1.2 (Steady state solution). *The unknown power demand (unmatched disturbance) P_d is constant and for a given P_d , there exist a \bar{u} and a state $(\bar{\eta}, \bar{\omega}, \bar{V}, \bar{P}_t, \bar{P}_g)$ that satisfies*

$$\begin{aligned} \mathbf{0} &= \mathcal{B}^T \bar{\omega} \\ \mathbf{0} &= -\bar{\omega} + K_p(\bar{P}_t - P_d - \mathcal{B}\Gamma(\bar{V}) \sin(\bar{\eta})) \\ \mathbf{0} &= -(X_d - X'_d)E(\bar{\eta})\bar{V} + \bar{E}_f, \end{aligned} \quad (6.7)$$

and

$$\begin{aligned} \mathbf{0} &= -\bar{P}_t + \bar{P}_g \\ \mathbf{0} &= -K^{-1}\bar{\omega} - \bar{P}_g + \bar{u}. \end{aligned} \quad (6.8)$$

To state an incremental passivity property of (6.3), we make use of the following storage function (Trip et al. 2016), (De Persis and Monshizadeh 2017):

$$S_1(\eta, \omega, V) = \frac{1}{2}\omega^T T_p \omega + \frac{1}{2}V^T E(\eta)V, \quad (6.9)$$

that can also be interpreted as a Hamiltonian function of the system (Stegink et al. 2017).

Lemma 6.1.3 (Incremental cyclo-passivity of (6.3)). *System (6.3) with input P_t and output ω is a strictly output incrementally cyclo-passive system, with respect to the constant $(\bar{\eta}, \bar{\omega}, \bar{V})$ satisfying (6.7).*

Proof. For notational convenience we define $x = (\eta, \omega, V)$. Following the calculation in Chapter 2, evaluation of (note the use of a calligraphic \mathcal{S})

$$\mathcal{S}_1(x) = S_1(x) - S_1(\bar{x}) - \nabla S_1(\bar{x})^T(x - \bar{x}), \quad (6.10)$$

shows that $\mathcal{S}_1(x)$ satisfies (see Chapter 2)

$$\begin{aligned} \dot{\mathcal{S}}_1(x) &= -\omega^T K_p^{-1}\omega - \dot{V}^T T_V (X_d - X'_d)^{-1} \dot{V} \\ &\quad + (\omega - \bar{\omega})^T (P_t - \bar{P}_t), \end{aligned} \quad (6.11)$$

along the solutions to (6.3). ■

For the stability analysis in Section 6.4 the following technical assumption is needed on the steady state that eventually allows us to infer boundedness of solutions.¹

Assumption 6.1.4 (Steady state voltages and voltage angles). *Let $\bar{V} \in \mathbb{R}_{>0}^n$ and let differences in steady state voltage angles satisfy*

$$\bar{\eta}_k \in \left(-\frac{\pi}{2}, \frac{\pi}{2}\right) \quad \forall k \in \mathcal{E}. \quad (6.12)$$

Furthermore, for all $i \in \mathcal{V}$ it holds that

$$\frac{1}{X_{di} - X'_{di}} - B_{ii} - \sum_{k \sim \{i,j\} \in \mathcal{E}} \frac{B_{ij}(\bar{V}_i + \bar{V}_j \sin^2(\bar{\eta}_k))}{\bar{V}_i \cos(\bar{\eta}_k)} > 0 \quad (6.13)$$

The assumption above holds if the generator reactances are small compared to the line reactances and the differences in voltage (angles) are small (De Persis and Monshizadeh 2017). It is important to note that this holds for typical operation points of the power networks. The main consequence of Assumption 6.1.4 is that the incremental storage function S_1 now obtains a strict local minimum at a steady state satisfying (6.7).

Lemma 6.1.5 (Local minimum of S_1). *Let Assumptions 6.1.4 hold. Then, the incremental storage function S_1 has a local minimum at $(\bar{\eta}, \bar{\omega}, \bar{V})$ satisfying (6.7).*

Proof. Under Assumption 6.1.4, the Hessian of (6.9), evaluated at $(\bar{\eta}, \bar{\omega}, \bar{V})$, is positive definite (Chapter 3). Consequently, $S_1(\bar{\eta}, \bar{\omega}, \bar{V})$ is strictly convex. The incremental storage function (6.10) is defined as a Bregman distance (Bregman 1967) associated with (6.9) for the points (η, ω, V) and $(\bar{\eta}, \bar{\omega}, \bar{V})$. Due to the strict convexity of $S_1(\bar{\eta}, \bar{\omega}, \bar{V})$, (6.10) has a local minimum at $(\bar{\eta}, \bar{\omega}, \bar{V})$. ■

Remark 6.1.6 (Sliding mode control for different power network models). *The focus of this work is to achieve OLFC by distributed sliding mode control for the nonlinear power network, explicitly taking into account the turbine-governor dynamics. Equations (6.3) well represent power systems for the purpose of frequency regulation and are often further simplified by assuming constant voltages, leading to the so called ‘swing equations’. To the analysis in this chapter the incremental passivity property established above is essential, which has been derived for various other models, including microgrids. It is therefore expected that the presented approach can be straightforwardly applied to a wider range of models than the one we consider here.*

¹ In case boundedness of solutions can be inferred by other means, Assumption 6.1.4 can be omitted.

6.2 Frequency regulation and economic dispatch

In this section we recall, for convenience and to make this chapter consistent, the control objectives of optimal load frequency control, that we have considered before in Chapter 2 and Chapter 5. Before doing so, we first note that the steady state frequency deviation $\bar{\omega}$, is generally different from zero without proper adjustments of \bar{u} .

Lemma 6.2.1 (Steady state frequency). *Let Assumption 6.1.2 hold, then necessarily $\bar{\omega} = \mathbb{1}_n \omega^*$ with*

$$\omega^* = \frac{\mathbb{1}_n^T (\bar{u} - \bar{P}_d)}{\mathbb{1}_n^T (K_p^{-1} + K^{-1}) \mathbb{1}_n}, \quad (6.14)$$

where $\mathbb{1}_n \in \mathbb{R}^n$ is the vector consisting of all ones.

This leads us to the first objective, concerning the regulation of the frequency deviation.

Objective 6.2.2 (Frequency regulation).

$$\lim_{t \rightarrow \infty} \omega(t) = \mathbf{0}. \quad (6.15)$$

From (6.14) it is clear that it is sufficient that $\mathbb{1}_n^T (\bar{u} - \bar{P}_d) = 0$, to have zero frequency deviation at the steady state. Therefore, there is flexibility to distribute the total required generation optimally among the various control areas. To make the notion of optimality explicit we assign to every control area a strictly convex linear-quadratic cost function $C_i(P_{ti})$ related to the generated power P_{ti} :

$$C_i(P_{ti}) = \frac{1}{2} q_i P_{ti}^2 + r_i P_{ti} + s_i \quad \forall i \in \mathcal{V}. \quad (6.16)$$

Minimizing the total generation cost, subject to the constraint that allows for a zero frequency deviation can then be formulated as the following optimization problem:

$$\begin{aligned} \min \quad & \sum_{i \in \mathcal{V}} C_i(P_{ti}) \\ \text{s.t.} \quad & \mathbb{1}_n^T (\bar{u} - \bar{P}_d) = 0. \end{aligned} \quad (6.17)$$

The lemma below, which is identical to Lemma 5.2.3 makes the solution to (6.17) explicit:

Lemma 6.2.3 (Optimal generation). *The solution \bar{P}_t^{opt} to (6.17) satisfies*

$$\bar{P}_t^{opt} = Q^{-1} (\bar{\lambda}^{opt} - R), \quad (6.18)$$

where

$$\bar{\lambda}^{opt} = \frac{\mathbf{1}_n \mathbf{1}_n^T (\bar{P}_d + Q^{-1} R)}{\mathbf{1}_n^T Q^{-1} \mathbf{1}_n}, \quad (6.19)$$

and $Q = \text{diag}(q_1, \dots, q_n)$, $R = (r_1, \dots, r_n)^T$.

From (6.18) it follows that the marginal costs $Q\bar{P}_t^{opt} + R$ are identical. Note that (6.18) depends explicitly on the *unknown* power demand P_d . We aim at the design of a controller solving (6.17) without measurements of the power demand, leading to the second objective.

Objective 6.2.4 (Economic dispatch).

$$\lim_{t \rightarrow \infty} P_t(t) = \bar{P}_t^{opt}, \quad (6.20)$$

with \bar{P}_t^{opt} as in (6.18), without measurements of P_d .

In order to achieve Objective 6.2.2 and Objective 6.2.4 we refine Assumption 6.1.2 that ensures the feasibility of the objectives.

Assumption 6.2.5 (Existence of an optimal steady state). *Assumption 6.1.2 holds when $\bar{\omega} = \mathbf{0}$ and $\bar{P}_t = \bar{P}_g = \bar{P}_t^{opt}$, with \bar{P}_t^{opt} as in (6.18).*

Remark 6.2.6 (Varying power demand). *To allow for a steady state solution, the power demand (unmatched disturbance) is required to be constant. This is not needed to reach the desired sliding manifold discussed in the next section, but is required only to establish the asymptotic convergence properties in Objective 6.2.2 and Objective 6.2.4.*

6.3 Distributed sliding mode control

In Section 6.1 we discussed a passivity property of the power network (6.3), with input P_t and output ω . Unfortunately, the turbine-governor system (6.4) does not immediately allow for a passive interconnection, since (6.4) is a linear system with relative degree two, when considering $-\omega$ as the input and P_t as the output. To alleviate this issue we propose a *distributed* Suboptimal Second Order Sliding Mode (D-SSOSM) control algorithm that simultaneously achieves Objective 6.2.2 and Objective 6.2.4, by passifying (6.4) and by exchanging information on the marginal costs. As a first step (see also Remark 6.3.2 below), we augment the turbine-governor

dynamics (6.4) with a distributed control scheme, resulting in:

$$\begin{aligned} T_t \dot{P}_t &= -P_t + P_g \\ T_g \dot{P}_g &= -K^{-1}\omega - P_g + u \\ T_\theta \dot{\theta} &= -\theta + P_t - A\mathcal{L}^{com}(Q\theta + R). \end{aligned} \quad (6.21)$$

Here, $Q\theta + R$ reflects the ‘virtual’ marginal costs and \mathcal{L}^{com} is the Laplacian matrix corresponding to the topology of an underlying communication network. The diagonal matrix $T_\theta \in \mathbb{R}^{n \times n}$ provides additional design freedom to shape the transient response and the matrix A is suggested later to obtain a suitable passivity property. We note that $\mathcal{L}^{com}(Q\theta + R)$ represents the exchange information on the marginal costs among the control areas. To guarantee an optimal coordination of generation among *all* the control areas the following assumption is made:

Assumption 6.3.1 (Communication topology). *The graph corresponding to the communication topology is undirected and connected.*

Remark 6.3.2 (First order turbine-governor dynamics). *The rational behind this seemingly ad-hoc choice of the augmented dynamics is that for the controlled first order turbine-governor dynamics, where $u = \theta$ and $P_g = -K^{-1}\omega + \theta$, system*

$$\begin{aligned} T_t \dot{P}_t &= -P_t - K^{-1}\omega + \theta \\ T_\theta \dot{\theta} &= -\theta + P_t - K^{-1}Q\mathcal{L}^{com}(Q\theta + R), \end{aligned} \quad (6.22)$$

has been shown to be incrementally passive with input $-\omega$ and output P_t , and is able to solve Objective 6.2.2 and Objective 6.2.4 (Chapter 5 and (Trip and De Persis 2017b)). We aim at the design of u and A in (6.21), such that (6.21) behaves similarly as (6.22). This is made explicit in Lemma 6.4.2.

To facilitate the discussion, we recall some definitions that are essential to sliding mode control. To this end, consider system

$$\dot{x} = \zeta(x, u) \quad (6.23)$$

with $x \in \mathbb{R}^n$, $u \in \mathbb{R}^m$.

Definition 6.3.3 (Sliding function). *The sliding function $\sigma(x) : \mathbb{R}^n \rightarrow \mathbb{R}^m$ is a sufficiently smooth output function of system (6.23).*

Definition 6.3.4 (r -sliding manifold). The r -sliding manifold² is given by

$$\{x, u \in \mathbb{R}^n : \sigma(x) = L_\zeta \sigma(x) = \cdots = L_\zeta^{(r-1)} \sigma(x) = \mathbf{0}\}, \quad (6.24)$$

where $L_\zeta^{(r-1)} \sigma(x)$ is the $(r-1)$ -th order Lie derivative of $\sigma(x)$ along the vector field $\zeta(x, u)$. With a slight abuse of notation we also write $L_\zeta \sigma(x) = \dot{\sigma}(x)$.

Definition 6.3.5 (r -sliding mode). A r -order sliding mode is enforced from $t = T_r \geq 0$, when, starting from an initial condition $x(0) = x_0$, the state of (6.23) reaches the r -sliding manifold (6.24), and there remains for all $t \geq T_r$.

Note that the order of a sliding mode controller is identical to the order of the sliding mode that it is aimed at enforcing.

We now propose a sliding function $\sigma(\omega, P_t, P_g, \theta)$ and a matrix A for system (6.21), which will allow us to prove convergence to the desired state. The choices are motivated by the stability analysis in the next section, but are stated here for the sake of exposition. First, the sliding function $\sigma : \mathbb{R}^{4n} \rightarrow \mathbb{R}^n$ is given by

$$\sigma(\omega, P_t, P_g, \theta) = M_1 \omega + M_2 P_t + M_3 P_g + M_4 \theta, \quad (6.25)$$

where $M_1 > \mathbf{0}$, $M_2 \geq \mathbf{0}$, $M_3 > \mathbf{0}$ are diagonal matrices and $M_4 = -(M_2 + M_3)$. Therefore, $\sigma_i, i \in \mathcal{V}$, depends only on the locally available variables that are defined on node i , facilitating the design of a distributed controller (see Remark 6.3.7). Second, the diagonal matrix $A \in \mathbb{R}^{n \times n}$ is defined as

$$A = (M_2 + M_3)^{-1} M_1 Q. \quad (6.26)$$

By regarding the sliding function (6.25) as the output function of system (6.3), (6.21), it appears that the relative degree³ of the system is equal to 1. This implies that a first order sliding mode controller can be *naturally* applied (Utkin 1992) in order to attain in a finite time, the sliding manifold defined by $\sigma = \mathbf{0}$. Note however that the control input u appears in the first time derivative of the sliding function. Since the sliding mode controller will generate a discontinuous control signal, this leads potentially to a discontinuous control input to the governor. Then, in order to provide a continuous control input u to the governor, we also require $\dot{\sigma} = \mathbf{0}$. Therefore, the desired sliding manifold is given by:

$$\{(\eta, \omega, V, P_t, P_g, \theta) : \sigma = \dot{\sigma} = \mathbf{0}\}. \quad (6.27)$$

We continue by discussing a possible controller attaining the desired sliding manifold (6.27) while providing a continuous control input u .

²For the sake of simplicity, the order r of the sliding manifold is omitted in the following.

³ The relative degree is the minimum order ρ of the time derivative $\sigma_i^{(\rho)}, i \in \mathcal{V}$, of the sliding function associated to the i -th node in which the control $u_i, i \in \mathcal{V}$, explicitly appears.

6.3.1 Suboptimal Second Order Sliding Mode controller

To prevent chattering, it is important to provide a continuous control input u to the governor. Since sliding mode controllers generate a discontinuous control signal, we adopt the procedure suggested in (Bartolini et al. 1998a) and first integrate the discontinuous signal, yielding for system (6.21):

$$\begin{aligned} T_t \dot{P}_t &= -P_t + P_g \\ T_g \dot{P}_g &= -K^{-1}\omega - P_g + u \\ T_\theta \dot{\theta} &= -\theta + P_t - A\mathcal{L}^{com}(Q\theta + R) \\ \dot{u} &= w, \end{aligned} \tag{6.28}$$

where w is the new (discontinuous) input generated by a sliding mode controller discussed below. A consequence is that the system relative degree (with respect to the new control input w) is now 2, and we need to rely on a second order ($r = 2$) sliding mode control strategy to attain the sliding manifold (6.25) in a finite time (Levant 2003). To make the controller design explicit, we discuss a specific second order sliding mode controller, the so-called ‘Suboptimal Second Order Sliding Mode’ (SSOSM) controller proposed in (Bartolini et al. 1998a). We introduce two auxiliary variables $\xi_1 = \sigma \in \mathbb{R}^n$ and $\xi_2 = \dot{\sigma} \in \mathbb{R}^n$, and define the so-called auxiliary system as:

$$\begin{cases} \dot{\xi}_1 = \xi_2 \\ \dot{\xi}_2 = \phi(\eta, \omega, V, P_t, P_g, \theta) + Gw. \end{cases} \tag{6.29}$$

Bearing in mind that $\dot{\xi}_2 = \ddot{\sigma} = \phi + Gw$, the expressions for the mapping ϕ and matrix G can be straightforwardly obtained from (6.25) by taking the second derivative of σ with respect to time, yielding for the latter⁴ $G = M_3 T_g^{-1} \in \mathbb{R}^{n \times n}$. We assume that the entries of ϕ and G have known bounds

$$|\phi_i| \leq \Phi_i \quad \forall i \in \mathcal{V} \tag{6.30}$$

$$0 < G_{\min_i} \leq G_{ii} \leq G_{\max_i} \quad \forall i \in \mathcal{V} \tag{6.31}$$

with Φ_i , G_{\min_i} and G_{\max_i} being positive constants. Second, w is a discontinuous control input described by the SSOSM control algorithm (Bartolini et al. 1998a), and consequently for each area $i \in \mathcal{V}$, the control law w_i is given by

$$w_i = -\alpha_i W_{\max_i} \operatorname{sgn} \left(\xi_{1_i} - \frac{1}{2} \xi_{1, \max_i} \right), \tag{6.32}$$

⁴The expression for ϕ is rather long and is omitted.

with

$$W_{\max_i} > \max \left(\frac{\Phi_i}{\alpha_i^* G_{\min_i}}; \frac{4\Phi_i}{3G_{\min_i} - \alpha_i^* G_{\max_i}} \right), \quad (6.33)$$

$$\alpha_i^* \in (0, 1] \cap \left(0, \frac{3G_{\min_i}}{G_{\max_i}} \right), \quad (6.34)$$

α_i switching between α_i^* and 1, according to (Bartolini et al. 1998a, Algorithm 1). Note that indeed the input signal to the governor, $u(t) = \int_0^t w(\tau) d\tau$, is continuous, since the input w is piecewise constant.

The extremal values ξ_{1, \max_i} in (6.32) can be detected by implementing for instance a peak detection as in (Bartolini et al. 1998b).

Remark 6.3.6 (Uncertainty of ϕ and G). *The mapping ϕ and matrix G are uncertain due to the presence of the unmeasurable power demand P_d and voltage angle θ , and possible uncertainties in the system parameters. In practical cases the bounds in (6.30) and (6.31) can be determined relying on data analysis and physical insights. However, if these bounds cannot be a-priori estimated, the adaptive version of the SSOSM algorithm proposed in (Incremona et al. 2016) can be used to dominate the effect of the uncertainties.*

Remark 6.3.7 (Distributed control). *Given A in (6.26), the dynamics of θ_i in (6.21) read for node $i \in \mathcal{V}$ as*

$$T_{\theta_i} \dot{\theta}_i = -\theta_i + P_i - \frac{Q_i M_{1ii}}{M_{2ii} + M_{3ii}} \sum_{j \in \mathcal{N}_i^{\text{com}}} (Q_i \theta_i + R_i - Q_j \theta_j - R_j), \quad (6.35)$$

where $\mathcal{N}_j^{\text{com}}$ is the set of controllers connected to controller i . Furthermore, (6.32) depends only on σ_i , i.e. on states defined at node i . Consequently, the overall controller is indeed distributed and only information on marginal costs needs to be shared among neighbours.

Remark 6.3.8 (Alternative SOSM controllers). *In this work we rely on the SOSM control law proposed in (Bartolini et al. 1998a). However, to constrain system (6.3) augmented with dynamics (6.28) on the sliding manifold (6.27), where $\sigma = \dot{\sigma} = \mathbf{0}$, any other SOSM control law that does not need the measurement of $\dot{\sigma}$ can be used. An interesting continuation of the presented results is to study the performance of various SOSM controllers within the setting of (optimal) LFC.*

Remark 6.3.9 (Relaxed conditions on the system parameters). *In comparison to the previous chapter, we do not require the parameters in (6.3) and (6.4) to satisfy Assumption 5.5.4.*

6.4 Stability analysis and main result

In this section we study the stability of the proposed control scheme, based on an enforced passivity property of (6.21) on the sliding manifold defined by (6.25). First, we establish that the second order sliding mode controller (6.29)–(6.34) constrains the system in finite time to the desired sliding manifold.

Lemma 6.4.1 (Convergence to the sliding manifold). *Let Assumption 6.1.1 hold. The solutions to system (6.3), augmented with (6.28), in closed loop with controller (6.29)–(6.34) converge in a finite time T_r to the sliding manifold (6.27) such that*

$$P_g = -M_3^{-1}(M_1\omega + M_2P_t + M_4\theta) \quad \forall t \geq T_r. \quad (6.36)$$

Proof. Following (Bartolini et al. 1998a), the application of (6.29)–(6.34) to each control area guarantees that $\sigma = \dot{\sigma} = \mathbf{0}$, $\forall t \geq T_r$. The details are omitted, and are an immediate consequence of the used SSOSM control algorithm (Bartolini et al. 1998a). Then, from (6.25) one can easily obtain (6.36), where M_3 is indeed invertible. ■

Exploiting relation (6.36), on the sliding manifold where $\sigma = \dot{\sigma} = \mathbf{0}$, the so-called equivalent system is as follows:

$$\begin{aligned} M_3T_t\dot{P}_t &= -(M_2 + M_3)P_t - M_4\theta - M_1\omega \\ T_\theta\dot{\theta} &= -\theta + P_t - \mathcal{AL}^{com}(Q\theta + R). \end{aligned} \quad (6.37)$$

As a consequence of the feasibility assumption (Assumption 6.1.2), the system above admits the following steady state:

$$\begin{aligned} \mathbf{0} &= -(M_2 + M_3)\bar{P}_t^{opt} - M_4\bar{\theta} - M_1\mathbf{0} \\ \mathbf{0} &= -\bar{\theta} + \bar{P}_t^{opt} - \mathcal{AL}^{com}(Q\bar{\theta} + R). \end{aligned} \quad (6.38)$$

Now, we show that system (6.37), with A as in (6.26), indeed possesses a passivity property with respect to the steady state (6.38). Note that, due to the discontinuous control law (6.32), the solutions to the closed loop system are understood in the sense of Filippov. Following the equivalent control method (Utkin 1992), the solutions to the equivalent system are however continuously differentiable.

Lemma 6.4.2 (Incremental passivity of (6.37)). *System (6.37) with input $-\omega$ and output P_t is an incrementally passive system, with respect to the constant $(\bar{P}_t^{opt}, \bar{\theta})$ satisfying (6.38).*

Proof. Consider the following incremental storage function

$$\begin{aligned} \mathcal{S}_2 = & \frac{1}{2}(P_t - \bar{P}_t^{opt})^T M_1^{-1} M_3 T_t (P_t - \bar{P}_t^{opt}) \\ & + \frac{1}{2}(\theta - \bar{\theta})^T M_1^{-1} (M_2 + M_3) T_\theta (\theta - \bar{\theta}), \end{aligned} \quad (6.39)$$

which is positive definite, since $M_1 > \mathbf{0}$, $M_2 \geq \mathbf{0}$ and $M_3 > \mathbf{0}$. Then, we have that \mathcal{S}_2 satisfies along the solutions to (6.37)

$$\begin{aligned} \dot{\mathcal{S}}_2 = & \frac{1}{2}(P_t - \bar{P}_t^{opt})^T M_1^{-1} M_3 T_t \dot{P}_t \\ & + \frac{1}{2}(\theta - \bar{\theta})^T M_1^{-1} (M_2 + M_3) T_\theta \dot{\theta} \\ = & \frac{1}{2}(P_t - \bar{P}_t^{opt})^T (-M_1^{-1} (M_2 + M_3) P_t - \omega - M_1^{-1} M_4 \theta) \\ & + \frac{1}{2}(\theta - \bar{\theta})^T M_1^{-1} (M_2 + M_3) (P_t - \theta - A\mathcal{L}^{com}(Q\theta + R)). \end{aligned}$$

In view of $M_4 = -(M_2 + M_3)$, $A = (M_2 + M_3)^{-1} M_1 Q$ and equality (6.38), it follows that

$$\begin{aligned} \dot{\mathcal{S}}_2 = & -(P_t - \theta)^T M_1^{-1} (M_2 + M_3) (P_t - \theta) \\ & - (Q\theta + R - Q\bar{\theta} - R) \mathcal{L}^{com}(Q\theta + R - Q\bar{\theta} - R) \\ & - (P_t - \bar{P}_t^{opt})^T (\omega - \mathbf{0}). \end{aligned}$$

■

Remark 6.4.3 (Reducing the relative degree). *An important consequence of the proposed sliding mode controller (6.29)–(6.34) is that the relative degree of system (6.37) is one with input $-\omega$ and output P_t . This is in contrast to the ‘original’ system (6.4) that has relative degree two with the same input–output pair.*

Now, relying on the interconnection of incrementally passive systems, we can prove the main result of this chapter concerning the evolution of the augmented system controlled via the proposed distributed SSOSM control strategy.

Theorem 6.4.4 (Main result: distributed OLFC). *Let Assumptions 6.1.1–6.3.1 hold. Consider system (6.3) and (6.21), controlled via (6.29)–(6.34). Then, the solutions of the closed-loop system starting in a neighbourhood of the equilibrium $(\bar{\eta}, \bar{\omega} = \mathbf{0}, \bar{V}, \bar{P}_t^{opt}, \bar{P}_g, \bar{\theta})$ approach the set where $\bar{\omega} = \mathbf{0}$ and $\bar{P}_t = \bar{P}_t^{opt}$, with \bar{P}_t^{opt} given by (6.18).*

Proof. Following Lemma 6.4.1, we have that the SSOSM control enforces system (6.21) to evolve $\forall t \geq T_r$ on the sliding manifold (6.27), resulting in the reduced order system (6.37). Consider the overall incremental storage function $\mathcal{S} = \mathcal{S}_1 + \mathcal{S}_2$, with \mathcal{S}_1 given by (6.10) and \mathcal{S}_2 given by (6.39). In view of Lemma 6.1.5, we have that \mathcal{S} has a local minimum at $(\bar{\eta}, \bar{\omega} = \mathbf{0}, \bar{V}, \bar{P}_t^{opt}, \bar{\theta})$ and satisfies along the solutions to (6.3), (6.37)

$$\begin{aligned} \dot{\mathcal{S}} &= -\omega^T K_p^{-1} \omega - \dot{V}^T T_V (X_d - X'_d)^{-1} \dot{V} \\ &\quad - (P_t - \theta)^T M_1^{-1} (M_2 + M_3) (P_t - \theta) \\ &\quad - (Q\theta + R - Q\bar{\theta} - R) \mathcal{L}^{com} (Q\theta + R - Q\bar{\theta} - R) \\ &\leq 0. \end{aligned}$$

Consequently, there exists a forward invariant set, Υ around $(\bar{\eta}, \bar{\omega} = \mathbf{0}, \bar{V}, \bar{P}_t^{opt}, \bar{\theta})$ and by LaSalle's invariance principle the solutions that start in Υ approach the largest invariant set contained in

$$\begin{aligned} \Upsilon \cap \{(\eta, \omega, V, P_t, \theta) : \omega = \mathbf{0}, V = ((X_d - X'_d)E(\bar{\eta}))^{-1} \bar{E}_f, \\ P_t = \theta, \theta = \bar{\theta} + Q^{-1} \mathbf{1}\alpha(t)\}, \end{aligned} \quad (6.40)$$

where $\alpha(t) \in \mathbb{R}$ is a scalar. On this invariant set the controlled power network satisfies

$$\begin{aligned} \dot{\eta} &= \mathcal{B}^T \mathbf{0} \\ \mathbf{0} &= K_p (\bar{\theta} + Q^{-1} \mathbf{1}\alpha(t) - P_d - \mathcal{B}\Gamma(V) \sin(\eta)) \\ \mathbf{0} &= -(X_d - X'_d)E(\eta)V + \bar{E}_f \\ M_3 T_t \dot{P}_t &= \mathbf{0} \\ T_\theta \dot{\theta} &= \mathbf{0}. \end{aligned} \quad (6.41)$$

Pre-multiplying both sides of the second line of (6.41) with $\mathbf{1}_n^T K_p^{-1}$ yields $0 = \mathbf{1}_n^T (\bar{\theta} + Q^{-1} \mathbf{1}\alpha(t) - P_d)$. Since $\bar{\theta} = \bar{P}_t^{opt}$, $\mathbf{1}_n^T (\bar{P}_t^{opt} - P_d) = 0$ and Q is a diagonal matrix with only positive elements, it follows that necessarily $\alpha(t) = 0$. We can conclude that the solutions to the system (6.3) and (6.21), controlled via (6.29)–(6.34), indeed approach the set where $\bar{\omega} = \mathbf{0}$ and $\bar{P}_t = \bar{P}_t^{opt}$, with \bar{P}_t^{opt} given by (6.18). ■

Remark 6.4.5 (Robustness to failed communication). *The proposed control scheme is distributed and as such requires a communication network to share information on the marginal costs. However, note that the term $-A\mathcal{L}^{com}(Q\theta + R)$ in (6.21) is not needed to enforce the passivity property established in Lemma 6.4.2, but is required to prove convergence to the economic efficient generation \bar{P}_t^{opt} . In fact, setting $A = \mathbf{0}$ still permits to infer frequency regulation following the argumentation of Theorem 6.4.4.*

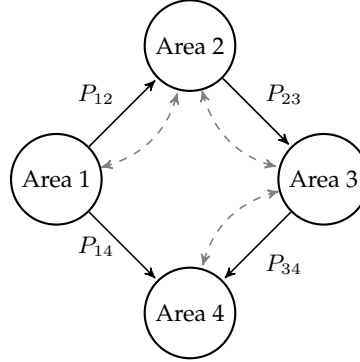


Figure 6.1: Scheme of the considered power network partitioned into 4 control areas, where $P_{ij} = B_{ij}V_iV_j \sin(\delta_i - \delta_j)$. The arrows indicate the positive direction of the power flows through the power network, while the dashed lines represent the communication network.

Remark 6.4.6 (Region of attraction). *LaSalle's invariance principle can be applied to all bounded solutions. As follows from Lemma 6.1.5, we have that the considered incremental storage function has a local minimum at the desired steady state, whereas the time to converge to the sliding manifold can be made arbitrarily small by properly choosing the gains of the SSOSM control. This guarantees that solutions starting in the vicinity of the steady state of interest remain bounded. A preliminary (numerical) assessment indicates that the region of attraction is large, but a thorough analysis is left as future endeavour.*

6.5 Case study

In this section, the proposed control solution is assessed in simulation, by implementing a power network partitioned into four control areas (e.g. the IEEE New England 39-bus system (Nabavi and Chakraborty 2013)). The topology of the power network is represented in Figure 6.1, together with the communication network (dashed lines). The line parameters are $B_{12} = -5.4$ p.u., $B_{23} = -5.0$ p.u., $B_{34} = -4.5$ p.u. and $B_{14} = -5.2$ p.u., while the network parameters and the power demand ΔP_{di} of each area are provided in Table 6.2, where a base power of 1000MW is assumed. The matrices in (6.25) are chosen as $M_1 = 3I_4$, $M_2 = I_4$, $M_3 = 0.1I_4$ and $M_4 = -(M_2 + M_3)$, $I_4 \in \mathbb{R}^{4 \times 4}$ being the identity matrix, while the control amplitude W_{\max_i} and the parameter α_i^* , $i = 1, \dots, 4$, in (6.32) are 10 and 1, respectively, for all $i \in \mathcal{V}$. For the sake of simplicity, in the cost function (6.16) we select $R_i = s_i = 0$

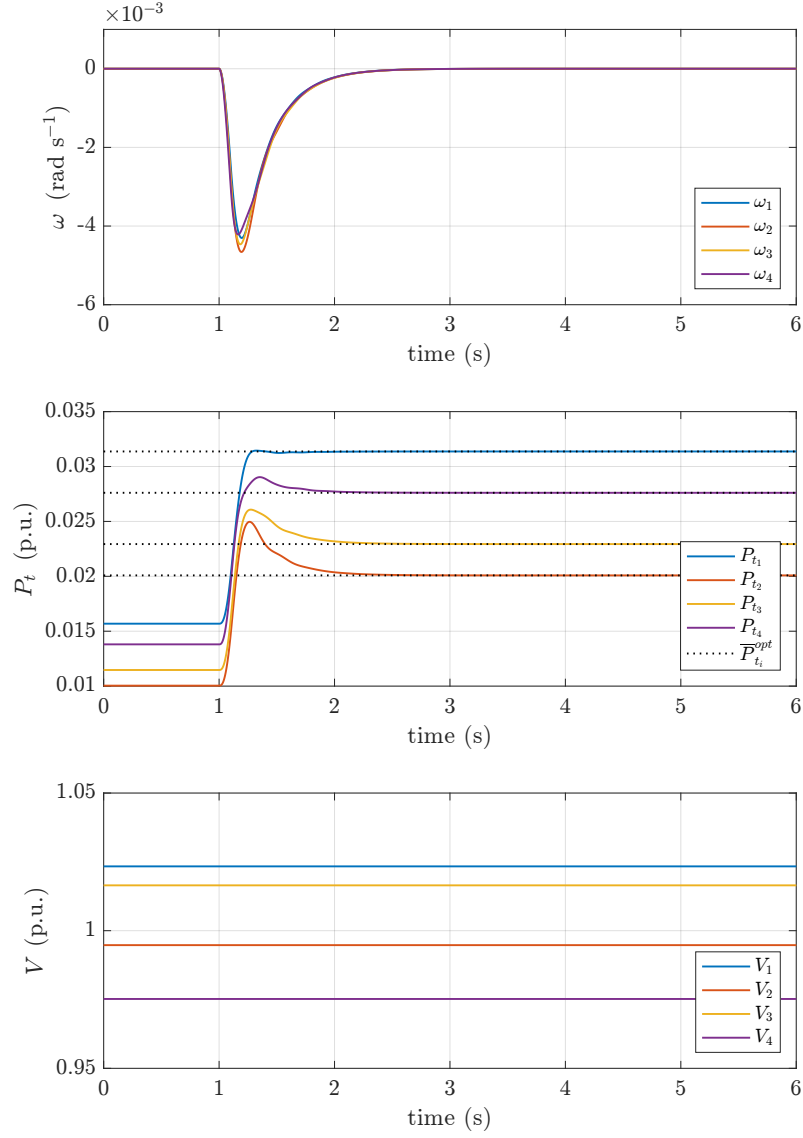


Figure 6.2: Time evolution of the frequency deviation, generated power and voltage dynamics considering a power demand variation at the time instant $t = 1$ s.

		Area 1	Area 2	Area 3	Area 4
T_{pi}	(s)	21.0	25.0	23.0	22.0
T_{ti}	(s)	0.30	0.33	0.35	0.28
T_{gi}	(s)	0.080	0.072	0.070	0.081
T_{Vi}	(s)	5.54	7.41	6.11	6.22
K_{pi}	(Hz p.u. ⁻¹)	120.0	112.5	115.0	118.5
K_i	(Hz p.u. ⁻¹)	2.5	2.7	2.6	2.8
X_{di}	(p.u.)	1.85	1.84	1.86	1.83
X'_{di}	(p.u.)	0.25	0.24	0.26	0.23
\overline{E}_{fi}	(p.u.)	1.0	1.0	1.0	1.0
B_{ii}	(p.u.)	-13.6	-12.9	-12.3	-12.3
$T_{\theta i}$	(s)	0.33	0.33	0.33	0.33
q_i	(\$ p.u. ⁻¹)	2.42	3.78	3.31	2.75
ΔP_{di}	(p.u.)	0.010	0.015	0.012	0.014

Table 6.2: Network Parameters and power demand

for all $i \in \mathcal{V}$. The system is initially at the steady state. Then, at the time instant $t = 1$ s, the power demand in each area is increased according to the values reported in Table 6.2. From Figure 6.2, one can observe that the frequency deviations converge asymptotically to zero after a transient where the frequency drops because of the increasing load. Indeed, one can note that the proposed controllers increase the power generation in order to reach again a zero steady state frequency deviation. Moreover, the total power demand is shared among the areas, minimizing the total generation costs. More precisely, by applying the proposed D-SSOSM, the total generation costs are 10 % less than the generation costs when each area would produce only for its own demand.

